Optimal multi-stage constant current charging pattern based on fire-fly algorithm for Li-ion battery

Guan-Jhu Chen[1*], Yong-Jie Chen[1], Jhan-Fong Lin[1]

Abstract— This paper introduces a novel approach for determining the optimal charging pattern (OCP) in the multi-stage constant current charging method. The primary objective of this technique is to minimize both the charging time and temperature increase during the charging process. To achieve this, a detailed equivalent circuit model (ECM) is employed to derive mathematical expressions for the charging time and charging loss of the battery. The fire-fly algorithm method is then utilized to simultaneously optimize the charging time and charging loss to identify the OCP. Experimental results demonstrate that the obtained OCP exhibits the lowest temperature rise and shortest charging time. A comparative analysis against the conventional CC-CV charging method using a 1C charging current reveals that the proposed method effectively improves the charging time, maximum temperature rise, and average temperature rise.

Keywords—Li-ion battery, battery charging, fire-fly algorithm

I. INTRODUCTION

The lithium-ion (Li-ion) battery is highly desirable due to its numerous advantageous properties, such as high energy density, lightweight design, extended cycle life, absence of memory effect, high operating voltage, and minimal self-discharge rate. Consequently, it is widely utilized in portable electronic devices, renewable energy systems, and electric vehicle energy storage devices. As power electronics technology continues to advance, research efforts are directed toward achieving faster charging speeds, prolonged battery cycle life, and enhanced charging efficiency. The most commonly employed charging technique for Li-ion batteries is constant current-constant voltage (CC-CV) charging. Initially, a constant current is applied to charge the battery, and as the battery voltage increases, a constant voltage is employed until it reaches the upper voltage limit (e.g., 4.2V). During this phase, the charging current is gradually reduced to a minimum value (e.g., 0.02C). However, the prolonged duration of the constant voltage charging stage leads to extended overall charging times and diminished cycle life. Hence, numerous studies have been conducted to enhance charging time, charging efficiency, and temperature regulation. In [1], a dual-loop control method is implemented to achieve constant current-constant voltage (CC-CV) charging without the need for measuring the charging current, thus reducing costs. [2] utilizes a fuzzy controller with inputs of battery open-circuit voltage and charging current to enhance the charging capacity during the constant voltage (CV) mode. Alternatively, in [3], a phase-locked loop control-based charging method is proposed, where the phase error is used as a reference to generate the charging current, resulting in a similar CC-CV charging pattern implemented through a different approach. To further enhance the performance of the phase-locked loop control, a current-pumped battery charger is introduced. In [4], the current-pumped charging technique is implemented for the constant current (CC) mode, while a pulsed current charging strategy is utilized for the constant voltage (CV) mode. This approach improves charging efficiency and achieves a comparable charging time to that of the CC-CV method. [5] proposes a grey-predicted Li-ion battery charge system, which reduces charging time and enhances charging efficiency compared to the conventional CC-CV charging technique. [6] and [7] employ a constant pulsed current for charging the battery, with the highest charging current achieved by adjusting the frequency or duty cycle of the pulse. On the other hand, in [8] and [9], pulsed current charging is employed, and the magnitude of the charging current can be modified by adjusting parameters such as pulse width and rest time, leading to various charging strategies. The multi-stage constant current (MSCC) charging method offers several advantages over the conventional constant current-constant voltage (CC-CV) charging technique, as supported by [10-12]. These advantages include ease of implementation, minimal temperature rise, and high charging efficiency. Moreover, the MSCC method has the potential to extend battery cycle life as it avoids the constant voltage (CV) mode, which subjects the battery to continuous stress. Instead, the MSCC charging technique utilizes multiple constant current (CC) stages with varying current amplitudes. The charging profile of the MSCC method comprises several CC stages, where each stage applies a specific current until a predetermined criterion is met.

The conditions for transitioning between stages in the multi-stage constant current charging method are primarily based on two factors: the upper limit of battery terminal voltage and the remaining battery capacity. Regarding the transition condition based on battery terminal voltage, [10] utilizes ant colony algorithm, while [11] employs particle

*Corresponding Author: Guan-Jhu Chen (E-mail:gjchen@ncut.edu.tw)
[1] Department of Electronic Engineering, National Chin-Yi University of Technology, No.57, Sec. 2, Zhongshan Rd., Taiping Dist., Taichung 411030, Taiwan (R.O.C.)

swarm optimization to search for the optimal current values for each stage of the five-stage charging process. This method requires extensive testing of multiple charging modes for a significant duration to determine the optimal current settings for each stage. However, it should be noted that this method is unable to fully charge the state of charge (SOC) to 100%.

In terms of the transition condition based on the remaining battery capacity, [12] utilizes the Taguchi method to find the optimal four-stage current settings. The switching stages are determined based on the battery's remaining capacity, specifically at 25%, 50%, and 75%. The remaining capacity is estimated using the Coulomb counting method combined with the battery's open circuit voltage. this paper uses battery voltage as the transition criterion for the MSCC charging technique. A voltage-based MSCC charging method is also easier to implement.

This study presents a novel approach for determining the open circuit potential (OCP) of the multi-stage constant current charging method, considering key performance indicators such as charging loss and charging time. The method combines the electrochemical model (ECM) of the Li-ion battery and the fire-fly algorithm (FA). Firstly, the electrochemical impedance spectroscopy (EIS) analysis is employed to construct an accurate battery ECM, enabling the derivation of mathematical expressions for charging loss and charging time. Secondly, the fire-fly algorithm (FA), a swarm intelligence method that balances exploration and exploitation, is utilized to simultaneously minimize charging loss and charging time, thereby identifying the optimal OCP for the MSCC charging method. Furthermore, a comparison with other charging methods is conducted to validate the effectiveness of the proposed approach. Experimental results demonstrate that the proposed method achieves a shorter charging time, higher charging efficiency, lower temperature rise, and longer battery cycle life. Moreover, compared to the conventional CC-CV charging technique, the proposed method exhibits significant improvements in maximum temperature rise and average temperature rise.

II. CHARGING STRATEGY

A. *The equivalent circuit model of the Li-ion battery*

This section introduces the Thevenin equivalent circuit model (ECM) for Li-Ion batteries, which is utilized to calculate the charge time, charge loss, and charge capacity in the context of the MSCC charging technique. The Thevenin circuit model consists of a battery capacitor (C_{eq}), a parallel resistor-capacitor circuit (R_p and C_p), and an internal resistor (R_o), as illustrated in Fig. 1. The R_p and C_p elements represent the battery's transient response, while the voltage on U_{Ceq} of C_{eq} corresponds to the open circuit voltage (OCV). Additionally, all ECM parameters are linked to the battery's state of charge (SOC), as shown in Fig 1.

Fig. 1 depicts the terminal voltage of the battery as V_{CT}, which serves as the cut-off voltage for the MSCC charging method. Based on Kirchhoff's voltage law, the equation for U_T can be expressed as Eq. (1), where $U_{Cp}(t) = U_{Rp}(t)$.

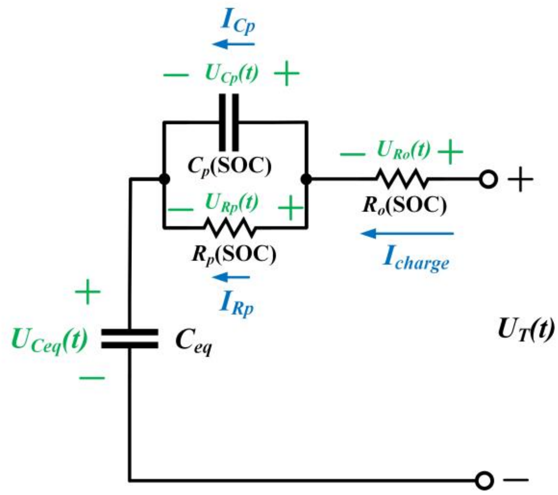

Figure 1 The equivalent circuit model of the battery

$$U_T(t) = U_{R_o}(t) + U_{R_p}(t) + U_{C_{eq}}(t) \tag{1}$$

To estimate the charging time of each charging stage, Eq. (3) can be derived from Eq. (2):

$$\Delta Q = C\Delta U = \int I\, dt = I \times \Delta t_s \tag{2}$$

$$\Delta t_s = \frac{C_{eq}}{I} \times \Delta U_s \tag{3}$$

where ΔU_s is the voltage drop caused by R_p and R_o.

In the MSCC charging technique, an assumption is made that the charging current frequency is zero, which implies that the impedance of the parallel capacitance is very high. Consequently, by assuming $I_{Rp} = I_{charge}$, Eq. (4) can be derived. The battery equivalent resistance, R_{eq}, in Eq. (4) is related to the state of charge (SOC) and can be represented by Eq. (5).

$$\Delta t_s = \frac{C_{eq}}{I_{charge,s}} \times \left[U_T - U_{C_{eq},s} - I_{charge,s} \times R_{eq}(SOC) \right] \tag{4}$$

$$R_{eq}(SOC) = R_o(SOC) + R_p(SOC) \tag{5}$$

Fig. 2 depicts the conceptual diagram of the MSCC method utilizing the battery ECM, where "s" indicates the stage number. $U_{Ceq,1}$ represents the initial voltage at SOC 0%, while ΔU_s represents the voltage drop across R_p and R_o. Each charging stage is associated with a voltage drop ΔU_1, ΔU_2, ΔU_3, ΔU_4, and ΔU_5, and the battery internal voltage $U_{Ceq,s}$ for each charging stage can be expressed as Eq. (6) to Eq. (9), respectively.

$$U_{Ceq,s} = U_T - \Delta U_s \text{ , } s = 1,2,3,4,5 \tag{6}$$

$$\begin{aligned} \Delta U_1 &= U_{C_{eq,2}} - U_{C_{eq,1}} \\ &= U_T - I_{charge,1} \times R_{eq}(SOC_2) - U_{C_{eq,1}} \end{aligned} \tag{7}$$

$$\begin{aligned} \Delta U_s &= U_{C_{eq,s+1}} - U_{C_{eq,s}} \text{ , } s = 2,3,4 \\ &= I_{charge,s-1} \times R_{eq}(SOC_s) - I_{charge,s} \times R_{eq}(SOC_{s+1}) \end{aligned} \tag{8}$$

$$\begin{aligned} \Delta U_5 &= U_T - U_{C_{eq,5}} \\ &= \left(U_T - I_{charge,5} \times R_{eq}(SOC_6)\right) \end{aligned} \tag{9}$$

where $I_{charge,s}$ represents the charging current of each stage.

Since the charging time of the multi-stage constant current charging method is determined by the charging current of each stage, the total charging time can be represented by Eq. (10) and Eq.(11).

$$T = \sum_{s=1}^{n} \Delta t_s \tag{10}$$

$$T_{total} = \sum_{s=1}^{n} \frac{C_{eq}}{I_{charge,s}} \times \Delta U_s \tag{11}$$

To charge the battery to 100%, the current value for the fifth stage can be calculated using Eq.(12).

$$I_{charge,5} = \frac{U_T - U_{Ceq,5}}{R_{eq}(SOC_5)} \tag{12}$$

where $U_{Ceq,5}$ represents the internal voltage of the battery after it is fully charged.

By using the aforementioned calculation method, the charging time for each charging stage can be determined. The charging energy loss can be expressed by the current value of each stage and the equivalent impedance corresponding to the SOC, as shown in Eq. (13) and (14).

$$L_{total}^{loss} = \sum_{s=1}^{n} \Delta L_s^{loss} \tag{13}$$

$$\Delta L_s^{loss} = \int_{t_{s-1}}^{t_s} I_{charge,s}^2 \times \left[R_{eq}\left(SOC(t)\right)\right] dt \tag{14}$$

B. *Electrochemical impedance spectroscopy*

The specifications of the lithium-ion battery used in this study are as follows. The test battery chosen for this study is the ICR18650-P28A lithium-ion battery manufactured by Molicel Corp [13]. The battery specifications are provided in Table 1.

The AC impedance analysis of lithium-ion batteries is primarily conducted using an AC impedance analyzer, which generates a set of variable-frequency sine wave voltage signals to perturb the battery. It is important to ensure that the perturbation voltage in constant voltage mode is not excessively large, as it may interfere with the battery's equilibrium state and result in measurement distortion. During active potentiostatic voltage perturbation detection, the perturbation voltage induces a corresponding current response. By detecting the amplitude and phase angle of the current, the current values are adjusted and converted. Finally, the impedance and phase angle difference are calculated based on the magnitude of the perturbation voltage and the corresponding current. This process is repeated until all the designated frequency ranges have been measured. Once the measurements for all frequencies are completed, AC impedance parameter analysis can be performed.

In this study, the Bio-Logic BCS-815 multi-channel charge-discharge system, in conjunction with the EC-Lab software interface, was used for AC impedance analysis. The selection of this equipment was based on considerations of battery equivalent model accuracy and experimental time requirements. The AC impedance analysis was conducted with a precision of 1% state of charge (SOC), and each measurement was followed by a battery rest period of 3 hours to ensure measurement accuracy

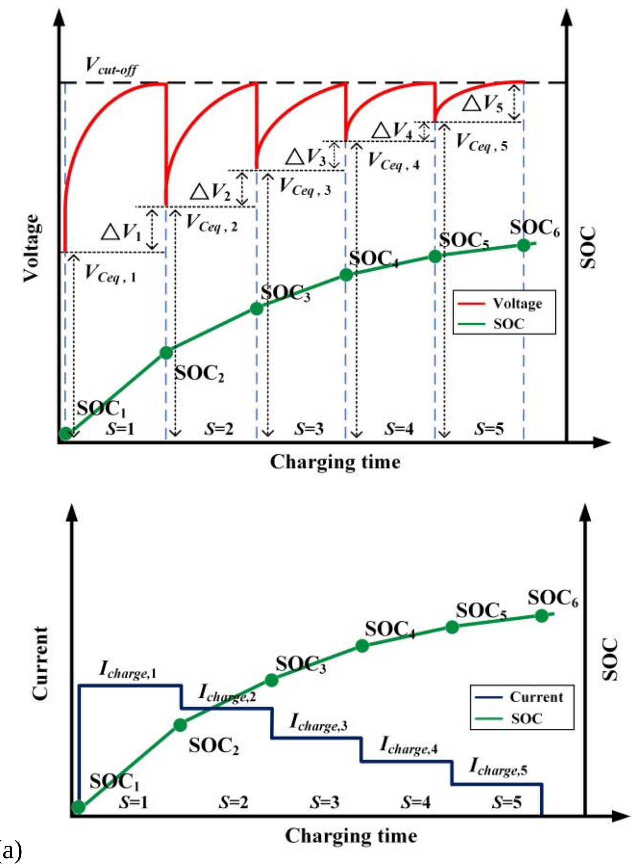

(a)

(b)

Figure 2 The schematic diagram of the MSCC charging method

Table 1 Molicel INR18650-P28A specifications

Nominal Capacity	2800 mAh
Nominal Voltage	3.6V
Cut-off Voltage	2.5 V
Standard Charge	CC-CV，2.8 mA，4.2 V
Dimension	18.4 mm (diameter) 65 mm (height)
Weight	46 g
Charge Temperature	0 ˚C to +60 ˚C
Discharge Temperature	-40 ˚C to +60 ˚C

C. Fire-fly algorithm -based OCP searching technique

The Fire-fly Algorithm (FA) was proposed by Yang et al. in 2009. This algorithm simulates the behavior of fireflies, which are attracted to each other based on their individual brightness. In nature, fireflies use brightness to find mates or prey. For modeling convenience, the algorithm assumes that all fireflies are gender-neutral, meaning that a firefly will be attracted to all other fireflies. The purpose of attraction in the algorithm is no longer to find a mate but solely to capture prey. The attraction between fireflies is directly proportional to their relative brightness. Fireflies with lower brightness are attracted to those with higher brightness, and they will move towards the brighter ones. Additionally, the attraction strength and brightness decrease as the distance between fireflies increases. When a firefly realizes that there are no other fireflies brighter than itself in the population, it will move randomly.

The luminosity formula of fireflies has evolved as a result of the evolutionary process, as illustrated from Equation 15 to Equation 17. By incorporating the inverse square law of brightness and distance, as well as the light absorption effect defined by Equation 15 and 16 , the luminosity formula can be derived into Equation 17.

$$I\left(r\right)=\frac{I_S}{r^2} \quad (15)$$

$$I=I_0\times e^{-\gamma r} \quad (16)$$

$$I\left(r\right)=I_0\times e^{-\gamma r^2} \quad (17)$$

Where I_s represents the luminosity of the brightest firefly individual, r is the distance between two fireflies, γ is the light absorption coefficient set to 0.01, and I_0 is the luminosity when the distance between two fireflies is 0.

The Firefly Algorithm transforms the luminosity (I) formula into the attractiveness (β) formula through Equation 18.

$$\beta=\beta_0\times e^{-\gamma r^2} \quad (18)$$

The detailed process of the algorithm is outlined in steps 1 to 7 as follows:

Step 1:Firefly Initialization, including initializing firefly positions (X) and firefly attractiveness (β).

Step 2: Set the current iteration count (i) equal to 1.

Step 3: Update the firefly positions using Equation X, where the firefly positions are influenced by attractiveness (β), distance ($X_k - X_j$), and the step length factor (α).

$$X_j\left(i+1\right)=X_j\left(i\right)+\beta_0\times e^{-\gamma r_{jk}^2}\times\left(X_k\left(i\right)-X_j\left(i\right)\right)+\alpha\times\varepsilon_j\left(i\right) \quad (19)$$

Where X_k and X_j represent the positions of firefly k and firefly j, respectively. r_{jk} is the distance between firefly j and firefly k. ε_j is a random vector for firefly j with values generated from either a Gaussian distribution or a uniform distribution, limited within the range [–0.5,0.5]. The step length factor α can be updated according to Equation 20.

$$\alpha=\alpha_0\times\theta\left(i\right) \quad (20)$$

In Equation 20, the scaling factor α_0 is set to 1, and the cooling factor θ typically falls within the range [0.95,0.99]. For this paper, it is set to 0.97.

Step 4: Update the firefly attractiveness using Equation 21.

$$\beta=\beta_0\times e^{-\gamma r^2} \quad (21)$$

Step 5: Evaluate the firefly fitness using the cost function equation.

Step 6: Check if the termination conditions are met. If they are met, proceed to step 7. If not, proceed to step 6A.

Step 6A: Let i=i+1, proceed to the next iteration, and return to Step 3.

Step 7: End the firefly algorithm process.

D. Cost function

Defining the cost function is indeed a critical step in implementing the Firefly Algorithm (FA) for optimization. In this study, the optimization objectives include charging loss and charging time, which are measured in different units. To enable fair comparison and effective optimization, a normalization method is proposed.

The fitness value in this study is computed based on the Euclidean distance between the obtained result and the ideal solution, as demonstrated in Fig 3. A smaller distance between these two points indicates a superior fitness value. The distance is mathematically expressed by Eq. (22) as illustrated in Fig 3:

$$d = \sqrt{\left(T_{now} - T_{min}\right)^2 + \left(L_{now} - L_{min}\right)^2} \tag{22}$$

To emphasize the significance of both parameters, a weighting factor α can be introduced, and Eq. (22) can be modified as Eq. (23), where T represents the charging time and L represents the charging loss:

$$Cost\ function = \sqrt{\alpha * \left(\frac{T_{now} - T_{min}}{T_{max} - T_{min}}\right)^2 + (1-\alpha) * \left(\frac{L_{now} - L_{min}}{L_{max} - L_{min}}\right)^2} \tag{23}$$

The minimum charging time can be achieved by employing a CC-CV charging method with a high charging current, whereas the minimum charging loss can be attained by utilizing a CC-CV charging method with a low charging current. MATLAB was employed to simulate the CC-CV charging method in this study. In Eq (16), (T_{max}, L_{min}) and (T_{min}, L_{max}) denote the charging time and charging loss, respectively, of the CC-CV charging method using 0.5C and 2C as the charging current.

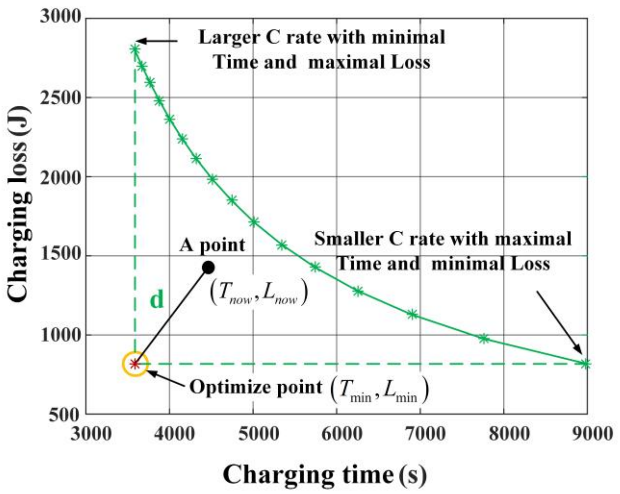

Figure 3 The concept diagram of fitness evaluation.

III. Simulation and Experiment Result

A. Simulation results

The Firefly Algorithm (FA) utilized in this study was configured with a maximum number of iterations set to 200. The battery used in this research is the Model INR18650-P28A Li-ion battery manufactured by Molicel Corp. The search space for the algorithm was defined as follows: for each stage of the MSCC charging technique, the current was restricted to a range between 0 C and 1 C. In this study, the cut-off voltage range was established as 4.2V~4.22V. Furthermore, a weighting value of 0.5 was assigned to Eq. (16), signifying equal significance placed on charging time and charging loss. To assess the efficiency and precision of the proposed method, four supplementary cases were simulated and implemented, along with a conventional CC-CV charging method, to verify the optimality of the obtained OCP. The simulation outcomes for each case are presented in Table 3.In Case 1, the OCP acquired through the proposed method is represented. Case 2 corresponds to a randomly selected result that deviates from the optimal solution. Case 3 is formed by increasing the values of I_1~I_4 in the obtained OCP by 0.1, whereas Case 4 is formed by decreasing the same values by 0.1. Case 5 is generated by fine-tuning the values. Nevertheless, when considering both the charging time and charging loss, the OCP obtained from the proposed method still demonstrates the highest fitness value.

B. Experimental results

Table 4 displays the experimental results, employing the same method settings as the simulations. These experimental findings align with the simulation results. The charging voltage and current curves for Case 1 and 1C-CCCV are shown in Fig. 4 and Fig. 5, respectively. To provide additional evidence of the effectiveness of the proposed method, this paper includes temperature rise curves of both the CC-CV charging method and the obtained OCP in Fig. 6. The experimental results indicate that, compared to the conventional CC-CV charging technique, the proposed method enhances the charging time, maximum temperature rise, and average temperature rise of the obtained OCP by 3.5%, 6.7%, and 12% respectively. Fig. 7 presents the temperature rise for all tested cases.

Table 3 The simulation results for each case.

	I_1	I_2	I_3	I_4	I_5	Time (sec)	Loss (J)	Fitness Value
1C-CCCV			2.8			5523	1708.2	0.354
Case 1	2.3632	1.6128	1.0500	0.7560	0.5113	4541	915.5	0.20863
Case 2	2.3548	1.6996	1.1648	0.8876	0.5113	4562	912.8	0.20948
Case 3	2.4632	1.7128	1.1500	0.8560	0.5113	4545	916.0	0.20922
Case4	2.2632	1.5128	0.9500	0.6560	0.5113	4719	877.4	0.21156
Case5	2.4632	1.5128	1.15	0.656	0.5113	4393	951.9	0.21175

Table 4 The experimental results for each case.

	Charge time	Avg. Temp (℃)	Max. Temp (℃)	Fitness
1C	4536	1.51	2.16	0.3585
Case 1	4377	1.41	1.90	0.3088
Case 2	4364	1.45	2.00	0.3210
Case 3	4177	1.49	2.10	0.3180
Case4	4499	1.39	1.75	0.3156
Case5	4139	1.58	2.02	0.3492

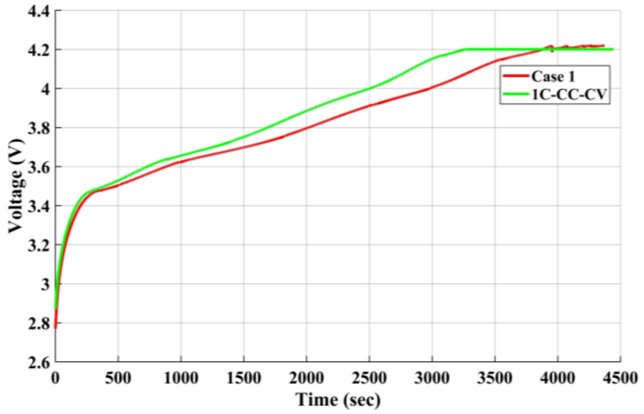

Figure 4 The voltage curves of Case1 to Case5

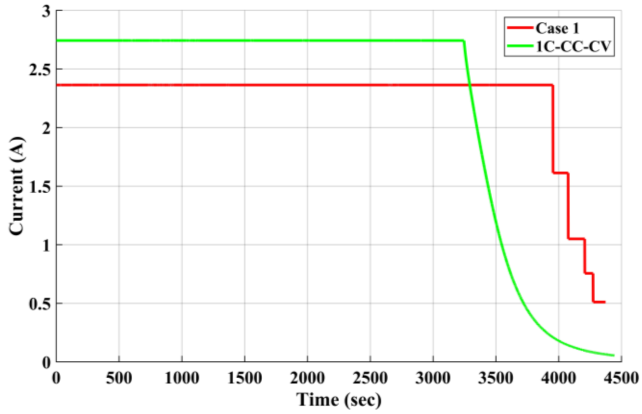

Figure 5 The current curves of Case1 to Case5

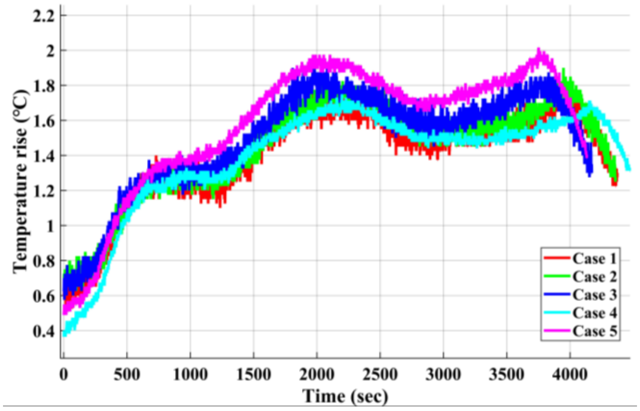

Figure 6 The temperature rise curves of Case1 to Case5

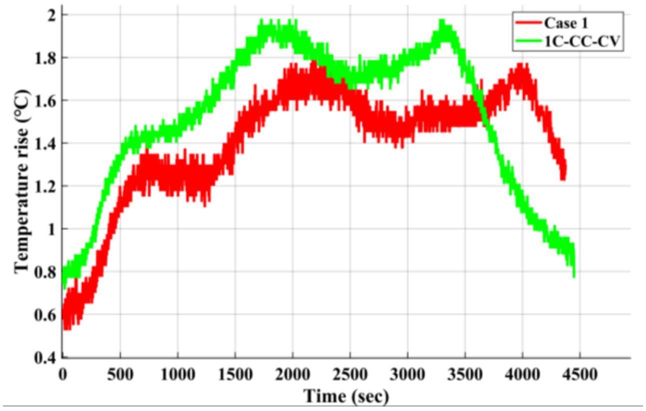

Figure 7 The temperature rise curves of Case1 and CC-CV charging method

IV. Conclusion

This study introduces a novel methodology for determining the optimal charging parameters (OCP) for the MSCC charging method. The approach leverages a comprehensive equivalent circuit model (ECM) of a Li-ion battery, obtained through electrochemical impedance spectroscopy (EIS) analysis, to calculate both the charging time and charging loss of the battery. The Fire-fly Algorithm (FA) is then utilized to identify the OCP that considers both the charging time and charging loss. The experimental results demonstrate that the proposed approach achieves the highest fitness value when considering both the charging time and charging loss. Moreover, compared to the conventional 1C CC-CV charging method, the proposed approach exhibits enhancements of 3.5% in charging time, 6.7% in average temperature rise, and 12% in maximum temperature rise.

References

[1] K.M. Tsang and W.L. Chan, "Current sensorless quick charger for lithiumion batteries," Energy Conversion and Management 52, pp.1593-1595, 2011.

[2] Guan-Chyun Hsieh, Liang-Rui Chen and Kuo-Sun Huang, "Fuzzy controlled Lithium-Ion Battery Charge System with Active State of Charge Controller," IEEE Transactions on Industrial Electronics, Vol. 48, No. 3, June 2001.

[3] Liang-Rui Chen, "PLL-Based Battery Charge Circuit Topology," IEEE Transactions on Industrial Electronics, Vol. 48, No. 3, June 2001.

[4] L. R. Chen, J. J. Chen, N. Y. Chu, and G. Y. Han, "Current pumped battery charger," IEEE Transactions on Industrial Electronics, vol. 55, no. 6, pp. 2482- 2488, Jun 2008.

[5] Liang-Rui Chen, Roy Chaoming Hsu and Chuan-Sheng Liu, "A Design of A Grey-Predicted Lithium-Ion Battery Charge System," IEEE Transactions on Industrial Electronics, Vol. 51, No. 6, June 2004.

[6] P.E. De Jongh and P.H.L. Notten, "Effect of Current Pulses on Lithium Intercalation Batteries," Solid State Ionics 148, pp. 259-268, June 2002.
[7] Jun Li, Edward Murphy, Jack Winnick and Paul A. Kohl, "The Effects of Pulse Charging on Cycling Characteristics of Commercial Lithium-Ion Batteries," Journal of Power Sources, vol. 102, pp. 302-309, Dec. 2001.
[8] L. R. Chen, "A design of an optimal battery pulse charge system by frequency-varied technique", IEEE Transactions on Industrial Electronics, vol. 54, no. 1, pp.398-405, Feb 2007.
[9] L. R. Chen, "A design of Duty-Varied Voltage Pulse Charger for Improving Lithium-Ion Battery-Charging Response", IEEE Transactions on Industrial Electronics, vol. 56, no. 2, pp.480-487, Feb. 2009.
[10] Search for an optimal rapid charging pattern for Li-ion batteries using ant colony system algorithm
[11] A PSO-based fuzzy-controlled searching for the optimal charge pattern of Li-ion batteries.
[12] Implementation of an SOC-based four-stage constant current charger for Li-ion batteries.
[13] Molicel Inc., "Lithium Ion Battery- Model INR18650-P28A," Specification of product.

Guan-Jhu Chen He obtained his Ph.D. in Electrical Engineering from the National Taiwan University of Science and Technology in Taipei, Taiwan, in 2021. He is currently in the Department of Electronic Engineering, National Chin-Yi University of Science and Technology, Taichung, Taiwan. His research interests include power electronics, digital power control and Li-ion battery charging algorithm.

Yong-Jie Chen was born in Tainan, Taiwan, R.O.C., in 2000. He received the B.S. degree in electronic engineering from National Chin-Yi University of Science and Technology (NCUT) in 2023. He is currently pursuing a M.S. degree in the department of Electronic Engineering at NCUT. His research interests include power electronics, and Li-ion battery charging algorithm.

Jhan-Fong Lin was born in Taichung, Taiwan, R.O.C., in 2001. He received the B.S. degree in electronic engineering from National Chin-Yi University of Science and Technology (NCUT) in 2023. He is currently pursuing a M.S. degree in the department of electronic engineering at NCUT. His research interests include power electronics, and optimization algorithm.